PI3 kinase and FOXO1 transcription factor activity differentially control B cells in the germinal center light and dark zones

Sander, S., Chu, V.T., Yasuda, T., Franklin, A., Graf, R., Calado, D.P., Li, S., Imami, K., Selbach, M., Di Virgilio, M., Bullinger, L., Rajewsky, K.

Immunity
2015 Dec 15 ; 43(6): 1075-1086
doi: 10.1016/j.immuni.2015.10.021
Publisher: Cell Press / Elsevier

PI3 Kinase and FOXO1 transcription factor activity differentially control B cells in the germinal center light and dark zones

Sandrine Sander [1*], Van Trung Chu [1], Tomoharu Yasuda [1], Andrew Franklin [1], Robin Graf [1], Dinis Pedro Calado [1,5], Shuang Li [1], Koshi Imami [2], Matthias Selbach [2], Michela Di Virgilio [3], Lars Bullinger [4] & Klaus Rajewsky [1*]

[1] Immune Regulation and Cancer, Max Delbrück Center for Molecular Medicine in the Helmholtz Alliance, Berlin-Buch 13125, Germany

[2] Proteome Dynamics, Max Delbrück Center for Molecular Medicine in the Helmholtz Alliance, Berlin-Buch 13125, Germany

[3] DNA Repair and Maintenance of Genome Stability, Max Delbrück Center for Molecular Medicine in the Helmholtz Alliance, Berlin-Buch 13125, Germany

[4] Department of Internal Medicine III, University Hospital Ulm, Ulm 89081, Germany

[5] Cancer Research UK, London Research Institute, London WC2A 3LY, UK; Peter Gorer Department of Immunobiology, Kings College London, London SE1 9RT, UK

* Correspondence:

Klaus Rajewsky, Immune Regulation and Cancer, Max-Delbrück-Center for Molecular Medicine in the Helmholtz Alliance, Robert-Rössle-Straße 10, 13125 Berlin, Germany. Phone: +49-30-9406-2391, Fax: +49-30-9406-3636, Email: klaus.rajewsky@mdc-berlin.de

Sandrine Sander, Immune Regulation and Cancer, Max-Delbrück-Center for Molecular Medicine in the Helmholtz Alliance, Robert-Rössle-Straße 10, 13125 Berlin, Germany. Phone: +49-30-9406-2391, Fax: +49-30-9406-3636, Email: sandrine.sander@mdc-berlin.de

Summary

Phoshpatidyl inositol 3' OH kinase (PI3K) signaling and FOXO transcription factors play opposing roles at several B cell developmental stages. We show here abundant nuclear FOXO1 expression in the proliferative compartment of the germinal center (GC), its dark zone (DZ), and PI3K activity, downregulating FOXO1, in the light zone (LZ), where cells are selected for further differentiation. In the LZ, however, FOXO1 was expressed in a fraction of cells destined for DZ reentry. Upon FOXO1 ablation or induction of PI3K activity, GCs lost their DZ, owing at least partly to downregulation of the chemokine receptor CXCR4. Although this prevented proper cyclic selection of cells in GCs, somatic hypermutation and proliferation were maintained. Class switch recombination was partly lost due to a failure of switch region targeting by activation-induced deaminase (AID).

Introduction

B cell differentiation is characterized by phases of cellular proliferation followed by periods during which the cells assume a resting state to further differentiate or persist in the system. An early period of proliferative expansion occurs in B cell progenitors in the bone marrow upon pre-B cell receptor expression (pre-BCR) (Reth and Nielsen, 2014). This event initiates a few rounds of division upon which the cells become resting small pre-B cells and differentiate into immature, BCR-expressing B cells. Upon transit into the peripheral immune system, some of these cells mature into resting peripheral B cells, which can persist for long periods of time. A second phase of cellular expansion occurs when mature B cells are driven into T-cell-dependent immune responses in a process called the germinal center (GC) reaction (Victora and Nussenzweig, 2012, Shlomchik and Weisel, 2012, Cyster, 2010, Zotos and Tarlinton, 2012, De Silva and Klein, 2015). In GCs, antigen-activated B cells undergo consecutive and cyclic phases of proliferation in the so-called GC dark zone (DZ), followed by a non-proliferative state in the GC light zone (LZ), where the cells are selected for DZ reentry or differentiation into memory B or plasma cells. Both pre-B cell differentiation in the bone marrow and the GC reaction in secondary lymphoid tissues involve genome editing in order to generate antibody diversity, through VDJ recombination in the former and somatic hypermutation (SHM) and class switch recombination (CSR) in the latter case. In both scenarios this is accompanied by stringent selection of

cells expressing appropriate antibody specificities. However, Recombination activating gene (RAG)-mediated VDJ recombination occurs in resting cells, whereas SHM takes place in proliferating GC cells, predominantly in the DZ. The site of CSR has not been firmly established.

Earlier work has identified two antagonistic players in the control of proliferation versus differentiation in pre-B cell development. Here, proliferative expansion is dependent on activation of phosphatidyl inositol 3' OH-Kinase (PI3K) signaling, which inhibits key transcription factors controlling cellular differentiation, namely Forkhead box transcription factors of the FOXO family, in keeping with the well-established role of FOXO transcription factors as tumor suppressors (Paik et al., 2007, Xie et al., 2012, Obrador-Hevia et al., 2012). Downregulation of PI3K activity and expression of FOXO transcription factors leads to the arrest of the cells in G1 phase and initiation of gene rearrangements at the IgL loci (Herzog et al., 2008). When the cells emerge from this differentiation process as mature, resting B cells, a BCR dependent "tonic" PI3K survival signal associated with downmodulation of FOXO1, becomes of vital importance (Srinivasan et al., 2009). Thus, at different stages of B cell differentiation and in a dose-dependent manner PI3K signaling can promote either cellular proliferation or survival, in accord with a large body of evidence obtained in other cell types (Engelman et al., 2006, Vanhaesebroeck et al., 2010, Thorpe et al., 2015).

Activation of PI3K signaling through ablation of its antagonist Phosphatase and tensin homolog (Pten), or indeed *Foxo1* deletion in mature B cells, interferes with CSR in T-cell-dependent antibody responses in vivo and activated B cells in vitro

(Suzuki et al., 2003, Omori et al., 2006, Dengler et al., 2008). Similarly, CSR is enhanced in activated B cells in culture by PI3K inhibition (Omori et al., 2006). There is suggestive evidence that these regulatory processes operate through the control of activation-induced deaminase (AID) expression by FOXO proteins. This earlier work implicates a regulatory role of FOXO1 in mature B cells but failed to address the interplay of PI3K signaling and FOXO1 in the GC reaction.

In brief, and in stark contrast to the situation in pre-B and mature B cells, we here report a crucial role for FOXO1 in the formation and/or maintenance of the GC DZ where GC B cells classically proliferate and undergo SHM. Upon GC B-cell-specific FOXO1 ablation or enforced PI3K activity, GCs developed, but lacked a discernible DZ. Although AID expression was not affected and SHM was only mildly reduced, CSR was largely ablated and the proper selection of high-affinity somatic antibody mutants was strongly disturbed. Together these findings indicate that the differential activation of PI3K and FOXO1 in mature B cells entering the GC reaction governs the sequence of proliferation, differentiation and selection processes in this microenvironment.

Results

DZ and LZ GC B Cells Display Differential PI3K and FOXO1 Activity

To study PI3K and FOXO1 activity in GCs, we immunized mice in which expression of a YFP reporter is initiated in GC B cells (*Cγ1-cre*, R26 *YFP*^{stopfl})

(Casola et al., 2006), with sheep red blood cells (SRBCs) and analyzed the GC response in the spleens of these animals 10 days later. Immunofluorescence and intracellular flow cytometry analysis revealed polarized PI3K signaling pathway activity in GCs: pAKT (S473) expression, which serves as a readout of active PI3K, was selectively increased in LZ compared to DZ cells (Figures 1A and 1B). The specificity of the pAKT antibody was demonstrated in control experiments where a pAKT (S473) blocking peptide abrogated antibody binding. In contrast, FOXO1 localized predominantly to the nucleus of DZ cells and was hardly detectable in most cells of the LZ (Figure 1C). Co-staining for surface IgM showed that the vast majority of FOXO1-expressing cells were indeed GC B cells (Figure S1A).

Thus, PI3K activity is largely restricted to B cells in the GC LZ; and the proliferating DZ B cells abundantly express nuclear FOXO1.

GC B cells Can Be Detected in Conditional Mouse Models of Constitutive PI3K Activation or FOXO1 Ablation

To directly address the functional role of PI3K signaling and FOXO1 in the GC reaction, we took advantage of a conditional mouse model that allowed the ablation of FOXO1 (Paik et al., 2007) and activation of a *YFP* reporter gene in early GC B cells. In parallel, we analyzed animals in which PI3K signaling was induced in GC B cells by expression of a constitutively active form of the catalytic PI3K subunit P110α (called *P110**) coupled to GFP via an internal ribosome entry site (IRES) sequence (Srinivasan et al., 2009) or enhanced by cre-

mediated ablation of Pten (Lesche et al., 2002), monitored by Rosa26-dependent YFP expression.

At 10 and 20 days after SRBC immunization, GC B cells were identified by flow cytometry ($CD19^{pos}$, $B220^{pos}$, $CD38^{low}$ and FAS^{high}) in the spleens of *Cγ1-cre*, R26 YFP^{stopfl} (Control), *Cγ1-cre,* R26 $P110^{*stopfl}$ (*P110**), *Cγ1-cre*, $Pten^{fl/fl}$, R26 YFP^{stopfl} ($Pten^{fl/fl}$) and *Cγ1-cre*, $Foxo1^{fl/fl}$, R26 YFP^{stopfl} ($Foxo1^{fl/fl}$) animals (Figure 1D). The proportions of reporter-positive cells within the GC B cell gate as well as the percentages and absolute numbers of GC B cells in mutant (i.e., *P110**, $Pten^{fl/fl}$ and $Foxo1^{fl/fl}$) compared to control animals did not reveal adverse effects of PI3K activation or *Foxo1* deletion on the overall GC reaction (Figures 1E, 1F and Figures S1B and S1C). We also found that *Foxo1* deletion in reporter gene-expressing GC B cells was highly efficient (Figure S1D) and did not lead to significant upregulation of *Foxo3* or *Foxo4* mRNA (Figure S1E). Similarly, in Peyer's patches GC B cell development or maintenance was not affected by PI3K activation or *Foxo1* deletion, with detection of reporter-positive cells at the expected lower frequency (Figures 1G and 1H; (Casola et al., 2006)).

Thus, constitutive PI3K activation or FOXO1 inactivation at an early stage of GC formation does not interfere with the generation of GC B cells.

GC DZ Formation Depends on PI3K Inactivation and Nuclear FOXO1

In contrast to the normal overall numbers of GC B cells, DZ and LZ compartmentalization was profoundly disturbed in the mutant animals both in

splenic GCs formed upon immunization and chronic GCs in Peyer's patches (Figures 2A, 2B and 2C). CD86 and CXCR4 expression serve as established markers to define the two compartments by flow cytometry analysis (Victora et al., 2012). In control animals DZ cells outnumbered LZ cells as previously described (Victora et al., 2010). In contrast, the splenic GC B cell compartment of immunized *P110** and *Foxo1*$^{fl/fl}$ animals consisted solely of CXCR4^{low}, CD86^{high} LZ-like cells. In PTEN-deficient splenic GC B cells a DZ-like population (CXCR4^{high}, CD86^{low}) was detectable, but the majority of the cells expressed low amounts of CXCR4, reminiscent of LZ cells. The leaky phenotype in these animals was not due to cells that had escaped *Pten* deletion (Figure S2A). In Peyer's patch GCs of *Foxo1*$^{fl/fl}$ and *P110** mutants essentially all reporter-positive B cells exhibited a LZ-like phenotype (Figure 2C).

The flow cytometry results were extended by gene expression profiling (GEP) analysis. In DZ and LZ cells from three immunized control animals (day 10 after SRBC injection) we identified 774 differentially regulated probe sets (corresponding to 584 genes) by a class comparison analysis ($p<0.01$; paired t test with random variance model; Table S2). The correct assignment of independent DZ and LZ samples (Victora et al., 2012) validated the relevance of these genes (Figure S2B). In a hierarchical cluster analysis based on the newly generated gene signature *P110**-expressing and FOXO1-deficient GC B cells resembled more closely LZ than DZ cells (Figure 2D). Indeed, about 2/3 of the DZ-associated gene program (511 out of 774 probe sets corresponding to 206 out of 584 genes) was lost in the mutant cells (Table S2), although their

expression profile was also clearly different from that of normal LZ cells (Figures S2C). For PTEN-deficient GC B cells, the small population of DZ-like cells may be responsible for their overall clustering more closely to DZ cells (Figure 2D). The supervised clustering was not exclusively dependent on the proliferative activity of the cells as removal of proliferation-associated genes (n = 106) from the signature did not change the clustering pattern (Figure S2D). Gene Set Enrichment Analysis (GSEA) showed that the normal DZ transcriptional program is highly enriched in FOXO1-proficient versus -deficient GC B cells (Figure 2E). Within the genes differentially regulated between these cells (Table S3) we identified factors controling the premature exit of GC B cells (*Bach2*, *Prdm1*, *Irf4*) (De Silva and Klein, 2015). In the absence of FOXO1, *Bach2* was reduced and thus expression of the master regulator of plasma cell differentiation *Prdm1* increased. In vitro activation of mutant cells confirmed previous reports (Dengler et al., 2008) demonstrating increased plasma cell differentiation in FOXO1-deficient B cells compared to controls (Figure S2E). As in LZ cells, *Irf4* expression was upregulated in FOXO1-ablated GC B cells, suggesting an additional mechanism of FOXO1-mediated GC maintenance control. In contrast, DNA-repair-associated genes (like Fanconi gene family members, *Brca1* and *Neil1*) were downregulated. Some of these genes have previously been linked to GC programs like DNA editing and B cell expansion (Nguyen et al., 2014, Mori et al., 2009, Bjorkman et al., 2015).

Histologically, in the GCs of *P110** and *Foxo1*$^{fl/fl}$ animals, the network of activated follicular dendritic cells (FDCs), which precisely demarcates the LZ in control

animals, extended through the entire GC structure and was populated by GC B cells with nuclear FOXO1 being barely detectable (Figure 2F). These GCs thus lacked a histologically discernible DZ. The FDC network disturbance and absence of *Foxo1*-expressing cells was less pronounced in *Pten*$^{fl/fl}$ animals, recapitulating the intermediate phenotype of PTEN deficiency observed in the flow cytometry and GEP analyses.

Thus, the formation and/or maintenance of the GC DZ is dependent on FOXO1, and constitutive PI3K pathway activation or *Foxo1* deletion results in defective GC architecture.

GC B Cells with Enforced PI3K Signaling or FOXO1 Ablation Proliferate and Undergo SHM But Are Improperly Selected

Although B cell proliferation in normal GCs is largely restricted to the DZ, we detected abundant cell proliferation in GCs from the mutant animals through staining for Ki67, a marker exclusively expressed by cycling cells (Figure 3A). Bromodeoxyuridine (BrdU) pulse labeling and flow cytometry analysis in control and mutant animals 10 days after SRBC immunization revealed incorporation in a large fraction of *P110**-expressing and PTEN- or FOXO1-deficient GC B cells, while in GCs from control animals it was largely restricted to DZ cells (Figure 3B). Similarly, when we concomitantly induced proliferation and either *P110** expression or *Foxo1* deletion in B cells isolated from control and *P110** or *Foxo1*$^{fl/fl}$ animals through exposure to anti-CD40 antibody or lipopolysaccharide (LPS) in combination with interleukin 4 (IL4), mutant cells divided to the same

extent as control cells in vitro (Figures 3C and S3A). The percentage of living cells over time was also similar in cultures of mutant and control cells (Figure 3D). Cell cycle analysis of anti-CD40+IL4- and LPS+IL4-stimulated B cells showed similar proportions of cells in G1, S and G2/M and sub-G1 for the different genotypes (Figures S3B and S3C).

The proliferative activity of the GC B cells in the mutants was accompanied by SHM of their rearranged variable (V) region genes (Figures 4A and S4A), as monitored by sequence analysis of the intron downstream of J_H4 (Jolly et al., 1997) on days 10 and 20 after SRBC immunization. This was in accord with similar overall AID transcript and protein expression in mutant and control cells, exceeding more than 50-fold those in non-GC B cells (Figures 4B and 4C). Notably, however, the load of somatic mutations was consistently lower in the mutants compared to the controls, both in terms of numbers of mutations per mutated sequence and the fraction of unmutated sequences. Among the mutants, the PTEN-deficient cells were intermediate in terms of somatic mutations between the *P110** and *Foxo1*$^{fl/fl}$ mutants.

To directly address clonal recruitment and affinity maturation in PI3K-activated and FOXO1-deficient GC B cells we analyzed the response of mutant mice to the hapten 4-hydroxy-3-nitro-phenylacetyl (NP) coupled to chicken gamma globulin (CGG). In wild-type mice, this response is dominated by Igλ^+ antibodies expressing the V186.2 IgH chain, in which the W33L mutation serves as a marker for affinity selection (Allen et al., 1987). However, in *P110** and *Foxo1*$^{fl/fl}$ animals the strong selection of Igλ-expressing cells in the GC B cell pool after NP

antigen exposure was not detectable (Figure 4D), with a similar (low) frequency of Igλ^+ B cells in their GCs as in the overall population of follicular B cells (Figure S4B). Similarly, the percentage and absolute number of hapten-binding GC B cells was significantly reduced in mutant animals compared to controls (Figure 4E and S4C). Within this cell population, IgG1-expressing cells were almost absent in the mutants (Figure S4D) indicating defective CSR in the absence of *Foxo1* expression (see below). Because of the difference in the clonal composition of NP-induced GCs in control and mutant animals we decided to analyze the V_H*186.2* mutation load in individual hapten-binding GC B cells by single cell sorting and cDNA sequencing (Kaji et al., 2012). Non-synonymous and synonymous V_H*186.2* gene mutations were significantly reduced in mutant GC B cells compared to controls (Figure S4E), recapitulating the SHM defect after SRBC immunization (Figure 4A). However, W33L mutations of V_H*186.2* were clearly detectable in *P110**-expressing or FOXO1-deficient GC B cells (Figure 4F), indicative of selection of high-affinity cells.

The abnormal cellular selection and reduced accumulation of somatic mutations in PI3K-pathway-activated and FOXO1-deficient GC B cells over time was in agreement with the observation that these cells failed to express the chemokine receptor CXCR4 (Figure 2A), a protein essential for GC DZ formation and suggested to be required for the proper selection of somatic antibody mutants in the GC reaction (Allen et al., 2004, Bannard et al., 2013). An essential step in the selection of cells expressing high-affinity antibody mutants is the recruitment of LZ cells back into the GC DZ (Victora et al., 2010, Oprea and Perelson, 1997,

Gitlin et al., 2014). In previous work, we and others had identified these cells as a minority of LZ B cells, namely those expressing the transcription factor c-MYC (Calado et al., 2012, Dominguez-Sola et al., 2012). Analyzing the c-MYC$^+$ B cells in the GC LZ of immunized control mice by immunofluorescence, we found that around 60% of these cells were positive for FOXO1, in striking contrast to the paucity of FOXO1$^+$ cells in the GC LZ (Figures 5A and 5B). These findings suggest that it is in the c-MYC$^+$ cells in the LZ that the FOXO1-dependent DZ transcriptional program is initiated.

CSR Is Blocked in LZ-like GC B Cells with Enforced PI3K Signaling or FOXO1 Ablation

In contrast to SHM in PI3K and *Foxo1* mutant GC B cells, we hardly found immunoglobulin isotype-switched cells in these cell populations. In the SRBC response, splenic GC B cells underwent CSR predominantly to express IgG1 and IgG2, but GC cells expressing these isotypes at the cell surface were strongly reduced in the spleens of immunized mutant animals (Figures 6A, 6B and S5A). There was also a profound reduction of IgA-expressing GC B cells in the Peyer's patches of the mutants (Figure 6C). In contrast, switching to IgG3, minor in the anti-SRBC response, seemed hardly affected (Figure S5B).

CSR involves a synapse between the recombining switch regions and the initiation of transcription from promoters upstream of the switch regions involved. The corresponding so-called germ-line transcripts (GLTs) support the switch region targeting of AID to produce staggered single-strand DNA breaks through

which switch region recombination is accomplished (Chaudhuri et al., 2007, Pavri and Nussenzweig, 2011). As AID expression appeared undisturbed in the mutants (Figures 4B and 4C) and the downstream machinery of CSR seemed intact given the undisturbed switching to IgG3 (Figure S5B), we analyzed whether FOXO1 activity was required to regulate AID targeting to switch regions. Therefore, GLT transcription for the various isotypes in GC B cells from immunized mutant and control animals was assessed and GLT expression was compared to those of post-switch transcripts (PSTs) in the same samples. The results indicated similar or even higher GLTs in mutants compared to controls for the upstream region of Sμ (Figure 6D). In contrast, γ1 GLT expression tended to be reduced in all mutants (Figure 6E) and fewer γ2b GLTs were detectable in *P110** GC B cells compared to controls (Figure S5C), although the data exhibited substantial scatter in several instances. γ3 GLTs were not diminished in the mutants (Figure S5D). The PSTs of γ1, γ2b and γ3 in the mutant and control cells were in accord with the percentage of switched GC B cells as detected by flow cytometry (Figures 6E, S5C and S5D), suggesting a CSR defect upstream of DNA recombination in PI3K-activated or *Foxo1*-deleted GC B cells. In a second, more direct approach, we addressed whether PI3K activation or *Foxo1* deletion affected the targeting of the switch regions by AID, through sequence analysis of the DNA immediately upstream of such regions. This approach is based on the earlier discovery that in the switching process these stretches of DNA accumulate footprints of AID activity in the form of somatic mutations (Petersen et al., 2001, Nagaoka et al., 2002, Reina-San-Martin et al., 2003). Extensive

somatic mutation was indeed evident upstream of Sμ in the controls, but it was clearly reduced in the mutants, most prominently in FOXO1-ablated cells (Figure 7A). In all cases, the cytosine-targeted mutations on both the transcribed and non-transcribed strands demonstrated a strong AID hotspot sequence motif preference (i.e., AG<u>C</u>T, mutated base underlined) (Figure 7B), and the distribution of the mutations along the DNA was similar to earlier results (Figure 7C) (Xue et al., 2006). With respect to downstream switch regions, we detected substantial numbers of mutated sequences only for Sγ1, with a similar clear reduction of mutations in the various mutant cells (Figure S6). Together, these findings indicate that ablation of FOXO1 impairs AID targeting to particular switch regions.

Discussion

PI3K signaling and the expression of FOXO transcription factors, which PI3K activity antagonizes, have been shown to play opposing roles in pre-B cell development, with PI3K controlling proliferative expansion and FOXO1 playing a crucial role during pre-B cell differentiation through IgL chain gene rearrangements (Herzog et al., 2008). The results reported here establish distinct roles for PI3K and FOXO1 activity for a later phase of B cell expansion, diversification, and selection, namely the GC reaction. Paradoxically, however, in this case it is FOXO1 that was highly expressed and active in the proliferative

compartment (i.e., the GC DZ), and PI3K activity was largely restricted to the LZ where the cells are selected on the basis of antibody affinity for reentry into the DZ or differentiation into memory B or plasma cells. Although FOXO1 expression in highly proliferative cells is at odds also with its well-established role as a tumor suppressor (Paik et al., 2007, Xie et al., 2012, Obrador-Hevia et al., 2012), recent evidence attests to its ability to function as an oncogene in certain cellular contexts (Sykes et al., 2011, Naka et al., 2010). Of particular relevance in connection to the GC reaction are recurrent activating mutations of *FOXO1* in GC B-cell-derived lymphomas, where the mutant FOXO1 is resistant to PI3K inactivation (Trinh et al., 2013). It remained unclear from this work, however, whether *FOXO1* mutations and PI3K activation coexisted in the same cells. That this scenario is indeed possible is strongly supported by the detection of similar *Foxo1* mutations in a mouse model of Burkitt lymphoma, where constitutive PI3K activation cooperates with c-MYC overexpression in tumor development (Sander et al., 2012). It remains to be clarified how the concerted action of the usually antagonistic principles of PI3K and FOXO1 activation can drive lymphomagenesis.

In the GC reaction, the role of FOXO1 in the proliferating DZ cells was clearly distinct from the above scenario in that the PI3K pathway was largely downregulated in these cells. Therefore, if FOXO1 plays a role in the control of proliferation in these cells, it would be in concert with other signaling or transcriptional regulators. However, the genetic experiments of ablating FOXO1 or enforcing PI3K activity in GC B cells shed light on these considerations in that

these genetic manipulations preclude the formation of a GC DZ, but in contrast left basic features of the GC reaction intact which have been traditionally considered hallmarks of the GC DZ. Thus, we still observed extensive proliferative activity in GCs upon *Foxo1* deletion or enforced PI3K activity, and SHM of rearranged immunoglobulin V region genes was clearly active in the mutant cells, although the load of somatic mutations lagged behind that accumulating in wild-type GC cells. Thus, neither cellular expansion nor SHM in GCs requires a GC DZ or FOXO1 activity.

On the other hand, as our study addressed B-cell-autonomous functions of FOXO1, we have to conclude that this transcription factor plays a critical role in programing GC B cells to adopt a gene expression program that impinges on them and their cellular environment such that a GC DZ is formed. Our gene expression and gene set enrichment analysis suggests that FOXO1 indeed directly or indirectly controls a major part of the gene expression program that distinguishes DZ from LZ cells, even when cell-cycle-related genes are excluded from the analysis. While apart from some well-known candidate genes, the identification of the signaling and transcriptional pathways regulated by FOXO1 in the GC DZ (including its possible involvement in the control of phosphatase activity that limits BCR-mediated selection in most cycling GC B cells (Khalil et al., 2012)) will have to await functional experiments.

One critical downstream player emerging from the analysis is the chemokine receptor CXCR4. As a characteristic marker of B cells in the GC DZ, CXCR4 expression is entirely lost in the PI3K and *Foxo1* mutants, in line with evidence in

the literature that FOXO1 can directly or indirectly control CXCR4 expression (Potente et al., 2005, Dubrovska et al., 2012). Work by Bannard et al. (Bannard et al., 2013) has suggested that CXCR4 controls DZ reentry of LZ cells. Consequently, CXCR4 deficiency leads to an inability of GC B cells to reside in the GC DZ and thus to properly participate in the program of mutation and selection in GCs. Accordingly, they found impaired SHM in these cells, similar to what we find in the PI3K and *Foxo1* mutants. That clonal recruitment and selection of high-affinity cells in GCs is profoundly disturbed in the mutant mice became evident from the analysis of the anti-NP response, which is dominated in wild-type mice by Igλ^+ antibodies expressing the *V186.2* V_H gene. In the mutants, such cells represented a minority of the GC B cell population, and the number of hapten-binding cells was drastically reduced. Thus, although sequence analysis demonstrated some selection for cells expressing high-affinity NP-binding receptors, this process is clearly hampered in the mutants. While the details of this deficiency remain to be worked out, it seems likely that the absence of distinct consecutive phases of clonal expansion and selection of non-cycling cells in the mutant GCs contributes to this phenotype. Still, the principle that B cell maintenance requires BCR expression seems to hold in the GC B cells of the mutants, as we did not observe an accumulation of stop codons generated by somatic mutations in the IgH chain V region genes isolated from those cells (unpublished data).

In contrast to SHM, CSR was severely hampered in the PI3K and *Foxo1* mutants. Earlier work has identified FOXO1 as an essential regulator of CSR, but

its activity has been ascribed to the control of AID expression, as studied in mitogen and IL4 activated naive B cells in vitro (Dengler et al., 2008). We have reproduced these results in our own experiments (unpublished data), but found that PI3K activation or *Foxo1* deletion selectively in GC B cells in vivo did not affect AID transcript or protein expression, while still abolishing CSR. The detection of reduced *Aicda* transcripts in ex vivo GC B cells in which *Foxo1* deficiency had been initiated before the cells had encountered antigen (Dengler et al., 2008) exemplifies the need for developmental-stage-specific ablation of the transcription factor to study its physiologic function. Similarly, the reduced IgG3 serum concentration in *CD19-cre*, *Pten*$^{fl/fl}$ animals after antigen stimulation (Suzuki et al., 2003) might be due to an altered cellular program induced upon PI3K activation in B cells before they enter the GC reaction. Analyzing early processes in CSR, namely pre-switch transcription and AID-mediated somatic hypermutation of DNA stretches adjacent to switch regions in the IgH locus, we have provided evidence that FOXO1 plays a critical, though possibly not exclusive, role in GC B cells in the initiation of CSR, at a stage prior to the introduction of AID-mediated DNA breaks. This concept is further supported by earlier experiments in which CSR is still markedly inhibited in in vitro-activated PTEN-deficient B cells retroviraly transduced with *Aicda* (Omori et al., 2006). The present results raise the possibility that FOXO1 is involved in the assembly of a pre-switch synaptic complex (Wuerffel et al., 2007, Zarrin et al., 2007, Gostissa et al., 2014) in which the recombining switch regions are brought together to enable efficient AID targeting. Interestingly, in the case of Sμ this was

independent of switch region transcription. The strong reduction of isotype switching to IgG1 and IgA in the spleens and Peyer's patches, respectively, of the mutant animals, in the presence of normal IgG3 CSR in mutant splenic GC B cells is indicative of switch region and perhaps context-dependent functions of the PI3K pathway and FOXO1 in the control of CSR. Indeed, in the accompanying paper, *Dominguez-Sola et al.* (Dominguez-Sola et al., 2015) identify FOXO1 binding in enhancer regions mediating intra-chromosomal interactions at the IgH locus (Kieffer-Kwon et al., 2013) in human tonsillar B cells by ChIP-Seq experiments. Another as yet unresolved question, which our experiments indirectly address, is the nature of the cells in the GC where CSR takes place. Given that CSR in GCs is thought to be induced by T-cell-dependent B cell activation in the GC LZ (where most cells do not express FOXO1) and was not affected in CXCR4-deficient GC B cells (Bannard et al., 2013) (which do not reside in the GC DZ), we speculate that it may occur in the small population of c-MYC-expressing B cells in the LZ that are candidates for DZ reentry (Calado et al., 2012, Dominguez-Sola et al., 2012) and for a fraction of which our data indicate upregulation of FOXO1.

Experimental procedures

Mice and immunization

Cγ1-cre; R26 *P110**^{stopfl}; *Foxo1*^{fl}*; Pten*^{fl} and R26 *YFP* ^{stopfl} alleles have been described (Casola et al., 2006, Calado et al., 2012, Srinivasan et al., 2009, Paik et al., 2007, Lesche et al., 2002). Animals were bred in our mouse colonies at the Immune Disease Institute (Boston) and Max Delbrück Center (Berlin). For T cell–dependent immunization, 8- to 12-week-old mice were injected intravenously with $1x10^9$ SRBCs (Cedarlane) in PBS or intraperitoneally with 100μg alum-precipitated NP-CGG (Sigma). Animals were analyzed at day 10 or day 20 after immunization. All animal care and procedures were approved by the Institutional Animal Care and Use Committee (IACUC) of Harvard University and the Immune Disease Institute (03341), and the LaGeSo Berlin (G0273/11).

BrdU incorporation experiments

Animals were immunized with SRBC and 10 days later 1mg BrdU (BD PharMingen) was intraperitoneally injected. 3 hours after BrdU injection the animals were sacrified and splenocytes were analyzed by flow cytometry for BrdU incorporation (BrdU Flow Kit; BD PharMingen).

in vitro B cell activation

To induce cre recombinase expression and B cell activation CD43 depleted (Miltenyi) splenic B cells of control and mutant animals were cultured in the presence of 1µg/ml of anti-CD40 antibody (HM40-3, eBioscience) or 20µg/ml of LPS (Sigma) and 25ng/ml of IL4 (R&D Systems) for a maximum of 5 days. At day 0 cells were labeled with CellTrace Violet (LifeTechnologies) according to the manufacturer's protocol. For cell cycle analysis *in vitro* activated B cells were stained with propidium iodide (Sigma) after RNase A (Sigma) treatment.

Flow Cytometry and cell sorting

A detailed list of the antibodies is provided in Supplemental Information. In the analysis of hapten binding 4-hyroxy-3-nitro-5-iodophenylacetyl (NIP) was used instead of NP, because of its 10 times higher affinity to Igλ^+ anti-NP antibodies (Allen et al., 1987).

Immunofluorescence analysis

Spleen sections from immunized control and mutant animals were frozen in OCT (Sakura Finetek) and liquid nitrogen. Cryo-sections (7µm) were fixed with 4% paraformaldehyde for 15 minutes at room temperature (RT). Afterwards, the slides were washed with PBS and incubated with PBS/0.25% TritonX-100 for 15 minutes at RT (permeabilization). For blocking of unspecific antibody binding the sections were incubated with PBS/3%BSA/0.2% TritonX-100 for 1 hour at RT. The tissues were stained for 1 hour at RT (or overnight at 4°C) with anti-FOXO1

antibody (C29H4, Cell Signaling), anti-c-MYC Dylight® 488 (Y69, Abcam), anti-CD21/CD35 APC (7G6, BD PharMingen), anti-BCL6 PE (GI191E, eBioscience), anti-Ki67 (MIB-5, Dako), anti-IgM APC (II/41, BD PharMingen), anti-FDC-M2 Alexa 546, and anti-IgD Cy5. Secondary goat-anti rabbit IgG-Alexa 488 and 546 antibodies (Invitrogen) were used if necessary. Nuclei were stained with DAPI. The sections were analyzed on a KEYENCE microscope.

Quantitative RT-PCR

Total RNA from sorted cells was extracted using the AllPrep DNA/RNA Kit (QIAgen) and cDNA was synthesized using random hexamer primers and the Thermoscript RT-PCR system (Invitrogen). For quantitative RT-PCR we used Power SYBR Green, followed by analysis with the StepOnePlus system (Applied Biosystems). Samples were assayed in triplicate and messenger abundance was normalized to that of *Hprt.* Primer sequences are provided in the Table S1.

Mass spectrometry based protein quantification

Proteins extracted from GC B cells of control and mutant animals (day 10 after SRBC immunization) were digested and subjected to online liquid chromatography-tandem mass spectrometry (nanoLC-MS/MS) analysis. A detailed description is provided in Supplemental Information.

IgH somatic mutation analysis

Genomic DNA was prepared from sorted GC B cells of SRBC immunized animals and the analysis was performed using published procedures (Jolly et al., 1997, Xue et al., 2006). Sequence analysis of the IgH region of NP specific GC B cells was performed as previously described (Kaji et al., 2012). Primer sequences are provided in the Table S1.

Statistical analysis

Data were analyzed using unpaired two-tailed student's t-test, Wilcoxon-Mann-Whitney test and Fisher's exact test, a p value ≤ 0.05 was considered significant.

Gene expression profiling and data analysis

Gene expression profiling was performed on GC B cell samples using Affymetrix GeneChip Mouse Genome 430 2.0 Arrays according to the manufacturer's recommendations (Affymetrix).

ACCESSION NUMBERS

The complete microarray data are available at the Gene Expression Omnibus (http://www.ncbi.nlm.nih.gov/projects/geo) under accession number GSE68043.

SUPPLEMENTAL INFORMATION

Supplemental information includes six figures, three tables and supplemental experimental procedures.

Author contributions:

S.S. and K.R. designed experiments and supervised all aspects of the project; S.S., V.T.C., T.Y., A.F., R.G., D.P.C., S.L., K.I., M.S., M.D.V. and L.B. did experiments and/or analyzed data. S.S. and K.R. wrote the manuscript and all authors discussed results and edited the manuscript.

Acknowledgements:

We thank R. A. DePinho (MD Anderson Cancer Center) for *Foxo1* $^{fl/fl}$ mice. We thank C. Grosse, J. Woehlecke, J. Pempe and K. Petsch for technical assistance; R. Lauhkonen-Seitz for administrative assistance; the Rajewsky laboratory members for critical comments and suggestions. We are grateful to R. Dalla-Favera and D. Dominguez-Sola for discussions and the communication of unpublished results. The work was supported by the Else Kröner-Fresenius-Stiftung (2014-A191 to S.S. and K.R.), the European Research Council (ERC Advanced Grant 268921 to K.R.) and the Deutsche Forschungsgemeinschaft (Heisenberg Scholarship BU 1339/3-1 to L.B.). M.D.V. is a Helmholtz Young Investigators Group leader (Helmholtz Association).

References

ALLEN, C. D., ANSEL, K. M., LOW, C., LESLEY, R., TAMAMURA, H., FUJII, N. & CYSTER, J. G. 2004. Germinal center dark and light zone organization is mediated by CXCR4 and CXCR5. *Nat Immunol,* 5**,** 943-52.

ALLEN, D., CUMANO, A., DILDROP, R., KOCKS, C., RAJEWSKY, K., RAJEWSKY, N., ROES, J., SABLITZKY, F. & SIEKEVITZ, M. 1987. Timing, genetic requirements and functional consequences of somatic hypermutation during B-cell development. *Immunol Rev,* 96**,** 5-22.

BANNARD, O., HORTON, R. M., ALLEN, C. D., AN, J., NAGASAWA, T. & CYSTER, J. G. 2013. Germinal center centroblasts transition to a centrocyte phenotype according to a timed program and depend on the dark zone for effective selection. *Immunity,* 39**,** 912-24.

BJORKMAN, A., QVIST, P., DU, L., BARTISH, M., ZARAVINOS, A., GEORGIOU, K., BORGLUM, A. D., GATTI, R. A., TORNGREN, T. & PAN-HAMMARSTROM, Q. 2015. Aberrant recombination and repair during immunoglobulin class switching in BRCA1-deficient human B cells. *Proc Natl Acad Sci U S A,* 112**,** 2157-62.

CALADO, D. P., SASAKI, Y., GODINHO, S. A., PELLERIN, A., KOCHERT, K., SLECKMAN, B. P., DE ALBORAN, I. M., JANZ, M., RODIG, S. & RAJEWSKY, K. 2012. The cell-cycle regulator c-Myc is essential for the formation and maintenance of germinal centers. *Nat Immunol,* 13**,** 1092-100.

CASOLA, S., CATTORETTI, G., UYTTERSPROT, N., KORALOV, S. B., SEAGAL, J., HAO, Z., WAISMAN, A., EGERT, A., GHITZA, D. & RAJEWSKY, K. 2006. Tracking germinal center B cells expressing germ-line immunoglobulin gamma1 transcripts by conditional gene targeting. *Proc Natl Acad Sci U S A,* 103**,** 7396-401.

CHAUDHURI, J., BASU, U., ZARRIN, A., YAN, C., FRANCO, S., PERLOT, T., VUONG, B., WANG, J., PHAN, R. T., DATTA, A., MANIS, J. & ALT, F. W. 2007. Evolution of the immunoglobulin heavy chain class switch recombination mechanism. *Adv Immunol,* 94**,** 157-214.

CYSTER, J. G. 2010. B cell follicles and antigen encounters of the third kind. *Nat Immunol,* 11**,** 989-96.

DE SILVA, N. S. & KLEIN, U. 2015. Dynamics of B cells in germinal centres. *Nat Rev Immunol,* 15**,** 137-48.

DENGLER, H. S., BARACHO, G. V., OMORI, S. A., BRUCKNER, S., ARDEN, K. C., CASTRILLON, D. H., DEPINHO, R. A. & RICKERT, R. C. 2008. Distinct functions for the transcription factor Foxo1 at various stages of B cell differentiation. *Nat Immunol,* 9**,** 1388-98.

DOMINGUEZ-SOLA, D., KUNG, J., HOLMES, A. B., WELLS, V. A., MO, T., BASSO, K. & DALLA-FAVERA, R. 2015. The FOXO1 Transcription Factor Instructs the Germinal Center Dark Zone Program. *Immunity*.

DOMINGUEZ-SOLA, D., VICTORA, G. D., YING, C. Y., PHAN, R. T., SAITO, M., NUSSENZWEIG, M. C. & DALLA-FAVERA, R. 2012. The proto-oncogene MYC is required for selection in the germinal center and cyclic reentry. *Nat Immunol,* 13**,** 1083-91.

DUBROVSKA, A., ELLIOTT, J., SALAMONE, R. J., TELEGEEV, G. D., STAKHOVSKY, A. E., SCHEPOTIN, I. B., YAN, F., WANG, Y., BOUCHEZ, L. C., KULARATNE, S. A., WATSON, J., TRUSSELL, C., REDDY, V. A., CHO, C. Y. & SCHULTZ, P. G. 2012. CXCR4 expression in prostate cancer progenitor cells. *PLoS One,* 7**,** e31226.

ENGELMAN, J. A., LUO, J. & CANTLEY, L. C. 2006. The evolution of phosphatidylinositol 3-kinases as regulators of growth and metabolism. *Nat Rev Genet,* 7**,** 606-19.

GITLIN, A. D., SHULMAN, Z. & NUSSENZWEIG, M. C. 2014. Clonal selection in the germinal centre by regulated proliferation and hypermutation. *Nature,* 509**,** 637-40.

GOSTISSA, M., SCHWER, B., CHANG, A., DONG, J., MEYERS, R. M., MARECKI, G. T., CHOI, V. W., CHIARLE, R., ZARRIN, A. A. & ALT, F. W. 2014. IgH class switching exploits a general property of two DNA breaks to be joined in cis over long chromosomal distances. *Proc Natl Acad Sci U S A,* 111**,** 2644-9.

HERZOG, S., HUG, E., MEIXLSPERGER, S., PAIK, J. H., DEPINHO, R. A., RETH, M. & JUMAA, H. 2008. SLP-65 regulates immunoglobulin light chain gene recombination through the PI(3)K-PKB-Foxo pathway. *Nat Immunol,* 9**,** 623-31.

JOLLY, C. J., KLIX, N. & NEUBERGER, M. S. 1997. Rapid methods for the analysis of immunoglobulin gene hypermutation: application to transgenic and gene targeted mice. *Nucleic Acids Res,* 25**,** 1913-9.

KAJI, T., ISHIGE, A., HIKIDA, M., TAKA, J., HIJIKATA, A., KUBO, M., NAGASHIMA, T., TAKAHASHI, Y., KUROSAKI, T., OKADA, M., OHARA, O., RAJEWSKY, K. & TAKEMORI, T. 2012. Distinct cellular pathways select germline-encoded and somatically mutated antibodies into immunological memory. *J Exp Med,* 209**,** 2079-97.

KHALIL, A. M., CAMBIER, J. C. & SHLOMCHIK, M. J. 2012. B cell receptor signal transduction in the GC is short-circuited by high phosphatase activity. *Science,* 336**,** 1178-81.

KIEFFER-KWON, K. R., TANG, Z., MATHE, E., QIAN, J., SUNG, M. H., LI, G., RESCH, W., BAEK, S., PRUETT, N., GRONTVED, L., VIAN, L., NELSON, S., ZARE, H., HAKIM, O., REYON, D., YAMANE, A., NAKAHASHI, H., KOVALCHUK, A. L., ZOU, J., JOUNG, J. K., SARTORELLI, V., WEI, C. L., RUAN, X., HAGER, G. L., RUAN, Y. & CASELLAS, R. 2013. Interactome maps of mouse gene regulatory domains reveal basic principles of transcriptional regulation. *Cell,* 155**,** 1507-20.

LESCHE, R., GROSZER, M., GAO, J., WANG, Y., MESSING, A., SUN, H., LIU, X. & WU, H. 2002. Cre/loxP-mediated inactivation of the murine Pten tumor suppressor gene. *Genesis,* 32**,** 148-9.

MORI, H., OUCHIDA, R., HIJIKATA, A., KITAMURA, H., OHARA, O., LI, Y., GAO, X., YASUI, A., LLOYD, R. S. & WANG, J. Y. 2009. Deficiency of the oxidative damage-specific DNA glycosylase NEIL1 leads to reduced germinal center B cell expansion. *DNA Repair (Amst),* 8**,** 1328-32.

NAGAOKA, H., MURAMATSU, M., YAMAMURA, N., KINOSHITA, K. & HONJO, T. 2002. Activation-induced deaminase (AID)-directed hypermutation in the immunoglobulin Smu region: implication of AID involvement in a common step of class switch recombination and somatic hypermutation. *J Exp Med,* 195**,** 529-34.

NAKA, K., HOSHII, T., MURAGUCHI, T., TADOKORO, Y., OOSHIO, T., KONDO, Y., NAKAO, S., MOTOYAMA, N. & HIRAO, A. 2010. TGF-beta-FOXO signalling maintains leukaemia-initiating cells in chronic myeloid leukaemia. *Nature,* 463**,** 676-80.

NGUYEN, T. V., RIOU, L., AOUFOUCHI, S. & ROSSELLI, F. 2014. Fanca deficiency reduces A/T transitions in somatic hypermutation and alters class switch recombination junctions in mouse B cells. *J Exp Med,* 211**,** 1011-8.

OBRADOR-HEVIA, A., SERRA-SITJAR, M., RODRIGUEZ, J., VILLALONGA, P. & FERNANDEZ DE MATTOS, S. 2012. The tumour suppressor FOXO3 is a key regulator of mantle cell lymphoma proliferation and survival. *Br J Haematol,* 156**,** 334-45.

OMORI, S. A., CATO, M. H., ANZELON-MILLS, A., PURI, K. D., SHAPIRO-SHELEF, M., CALAME, K. & RICKERT, R. C. 2006. Regulation of class-switch recombination and plasma cell differentiation by phosphatidylinositol 3-kinase signaling. *Immunity,* 25**,** 545-57.

OPREA, M. & PERELSON, A. S. 1997. Somatic mutation leads to efficient affinity maturation when centrocytes recycle back to centroblasts. *J Immunol,* 158**,** 5155-62.

PAIK, J. H., KOLLIPARA, R., CHU, G., JI, H., XIAO, Y., DING, Z., MIAO, L., TOTHOVA, Z., HORNER, J. W., CARRASCO, D. R., JIANG, S., GILLILAND, D. G., CHIN, L., WONG, W. H., CASTRILLON, D. H. & DEPINHO, R. A. 2007. FoxOs are lineage-restricted redundant tumor suppressors and regulate endothelial cell homeostasis. *Cell,* 128**,** 309-23.

PAVRI, R. & NUSSENZWEIG, M. C. 2011. AID targeting in antibody diversity. *Adv Immunol,* 110**,** 1-26.

PETERSEN, S., CASELLAS, R., REINA-SAN-MARTIN, B., CHEN, H. T., DIFILIPPANTONIO, M. J., WILSON, P. C., HANITSCH, L., CELESTE, A., MURAMATSU, M., PILCH, D. R., REDON, C., RIED, T., BONNER, W. M., HONJO, T., NUSSENZWEIG, M. C. & NUSSENZWEIG, A. 2001. AID is required to initiate Nbs1/gamma-H2AX focus formation and mutations at sites of class switching. *Nature,* 414**,** 660-5.

POTENTE, M., URBICH, C., SASAKI, K., HOFMANN, W. K., HEESCHEN, C., AICHER, A., KOLLIPARA, R., DEPINHO, R. A., ZEIHER, A. M. & DIMMELER, S. 2005. Involvement of Foxo transcription factors in angiogenesis and postnatal neovascularization. *J Clin Invest,* 115**,** 2382-92.

REINA-SAN-MARTIN, B., DIFILIPPANTONIO, S., HANITSCH, L., MASILAMANI, R. F., NUSSENZWEIG, A. & NUSSENZWEIG, M. C. 2003. H2AX is required for recombination between immunoglobulin switch regions but not for intra-switch region recombination or somatic hypermutation. *J Exp Med,* 197**,** 1767-78.

RETH, M. & NIELSEN, P. 2014. Signaling circuits in early B-cell development. *Adv Immunol,* 122**,** 129-75.

SANDER, S., CALADO, D. P., SRINIVASAN, L., KOCHERT, K., ZHANG, B., ROSOLOWSKI, M., RODIG, S. J., HOLZMANN, K., STILGENBAUER, S., SIEBERT, R., BULLINGER, L. & RAJEWSKY, K. 2012. Synergy between PI3K signaling and MYC in Burkitt lymphomagenesis. *Cancer Cell,* 22**,** 167-79.

SHLOMCHIK, M. J. & WEISEL, F. 2012. Germinal center selection and the development of memory B and plasma cells. *Immunol Rev,* 247**,** 52-63.

SRINIVASAN, L., SASAKI, Y., CALADO, D. P., ZHANG, B., PAIK, J. H., DEPINHO, R. A., KUTOK, J. L., KEARNEY, J. F., OTIPOBY, K. L. & RAJEWSKY, K. 2009. PI3 kinase signals BCR-dependent mature B cell survival. *Cell,* 139**,** 573-86.

SUZUKI, A., KAISHO, T., OHISHI, M., TSUKIO-YAMAGUCHI, M., TSUBATA, T., KONI, P. A., SASAKI, T., MAK, T. W. & NAKANO, T. 2003. Critical roles of Pten in B cell homeostasis and immunoglobulin class switch recombination. *J Exp Med,* 197**,** 657-67.

SYKES, S. M., LANE, S. W., BULLINGER, L., KALAITZIDIS, D., YUSUF, R., SAEZ, B., FERRARO, F., MERCIER, F., SINGH, H., BRUMME, K. M., ACHARYA, S. S., SCHOLL, C., TOTHOVA, Z., ATTAR, E. C., FROHLING, S., DEPINHO, R. A., ARMSTRONG, S. A., GILLILAND, D. G. & SCADDEN, D. T. 2011. AKT/FOXO signaling enforces reversible differentiation blockade in myeloid leukemias. *Cell,* 146**,** 697-708.

THORPE, L. M., YUZUGULLU, H. & ZHAO, J. J. 2015. PI3K in cancer: divergent roles of isoforms, modes of activation and therapeutic targeting. *Nat Rev Cancer,* 15**,** 7-24.

TRINH, D. L., SCOTT, D. W., MORIN, R. D., MENDEZ-LAGO, M., AN, J., JONES, S. J., MUNGALL, A. J., ZHAO, Y., SCHEIN, J., STEIDL, C., CONNORS, J. M., GASCOYNE, R. D. & MARRA, M. A. 2013. Analysis of FOXO1 mutations in diffuse large B-cell lymphoma. *Blood,* 121**,** 3666-74.

VANHAESEBROECK, B., GUILLERMET-GUIBERT, J., GRAUPERA, M. & BILANGES, B. 2010. The emerging mechanisms of isoform-specific PI3K signalling. *Nat Rev Mol Cell Biol,* 11**,** 329-41.

VICTORA, G. D., DOMINGUEZ-SOLA, D., HOLMES, A. B., DEROUBAIX, S., DALLA-FAVERA, R. & NUSSENZWEIG, M. C. 2012. Identification of human germinal center light and dark zone cells and their relationship to human B-cell lymphomas. *Blood,* 120**,** 2240-8.

VICTORA, G. D. & NUSSENZWEIG, M. C. 2012. Germinal centers. *Annu Rev Immunol,* 30**,** 429-57.

VICTORA, G. D., SCHWICKERT, T. A., FOOKSMAN, D. R., KAMPHORST, A. O., MEYER-HERMANN, M., DUSTIN, M. L. & NUSSENZWEIG, M. C. 2010. Germinal center dynamics revealed by multiphoton microscopy with a photoactivatable fluorescent reporter. *Cell,* 143**,** 592-605.

WUERFFEL, R., WANG, L., GRIGERA, F., MANIS, J., SELSING, E., PERLOT, T., ALT, F. W., COGNE, M., PINAUD, E. & KENTER, A. L. 2007. S-S synapsis during class switch recombination is promoted by distantly located transcriptional elements and activation-induced deaminase. *Immunity,* 27**,** 711-22.

XIE, L., USHMOROV, A., LEITHAUSER, F., GUAN, H., STEIDL, C., FARBINGER, J., PELZER, C., VOGEL, M. J., MAIER, H. J., GASCOYNE, R. D., MOLLER, P. & WIRTH, T. 2012. FOXO1 is a tumor suppressor in classical Hodgkin lymphoma. *Blood,* 119**,** 3503-11.

XUE, K., RADA, C. & NEUBERGER, M. S. 2006. The in vivo pattern of AID targeting to immunoglobulin switch regions deduced from mutation spectra in msh2-/- ung-/- mice. *J Exp Med,* 203**,** 2085-94.

ZARRIN, A. A., DEL VECCHIO, C., TSENG, E., GLEASON, M., ZARIN, P., TIAN, M. & ALT, F. W. 2007. Antibody class switching mediated by yeast endonuclease-generated DNA breaks. *Science,* 315**,** 377-81.

ZOTOS, D. & TARLINTON, D. M. 2012. Determining germinal centre B cell fate. *Trends Immunol,* 33**,** 281-8.

Figure legends

Figure 1. Compartmentalized Expression of Nuclear FOXO1 and pAKT in GCs, and Normal GC B Cell Frequencies in Genetically Modified Animals.

(A) Detection of pAKT (S473) in splenic DZ and LZ GC B cells of immunized control animals (day 10 after SRBC administration) by intracellular flow cytometry analysis. CD86 and CXCR4 surface marker stainings were included to define DZ ($CD86^{lo}CXCR4^{hi}$) and LZ ($CD86^{hi}CXCR4^{lo}$) cells. After fixation and permeabilization, splenocytes were incubated with pAKT (S473) antibody (antibody) or rabbit IgG (isotype control) or pAKT (S473) antibody plus pAKT (S473) blocking peptide (blocking peptide).

(B) Summary and quantification of flow cytometry data as shown in (A). Each symbol represents an individual animal; horizontal lines indicate the mean.

(C) Immunofluorescence analysis of spleen sections from immunized control animals (day 10 after SRBC injection). Antibodies detecting FOXO1, FDC-M2 (which delineates the activated FDC network) and IgD (which marks the follicular B cell compartment) were used. Dashed lines delineate DZ and LZ. Two individual animals were analyzed. Scale bars represent 25 μm. Graph: Summary and quantification of immunofluorescence analysis (presented as in B). Each symbol represents an individual GC.

(D) Representative flow cytometry analysis of splenocytes from immunized control and mutant animals (*P110**; $Pten^{fl/fl}$; $Foxo1^{fl/fl}$) at day 10 after SRBC

injection. Reporter gene expression was used to monitor cre-mediated recombination. Cells were consecutively gated on viable (TO-PRO-3^{-} or PI^{-}) lymphocytes, B cells (B220^{+}CD19^{+}) and GC B cells (CD38^{lo}FAS^{hi}). Numbers adjacent to outlined areas indicate the percentage of cells.

(E and F) Summary and quantification of flow cytometry data of reporter^{+} (E) and GC B (F) cells as shown in (D). Each symbol represents an individual animal; horizontal lines indicate the mean.

(G and H) Summary and quantification of flow cytometry data of reporter^{+} (G) and GC B (H) cells detected in Peyer's patches (presented as in E and F).

NS, not significant ($p > 0.05$); *$p \leq 0.05$ and **$p \leq 0.001$ (Wilcoxon-Mann-Whitney test). See also Figure S1.

Figure 2. PI3K-Pathway-Activated or *Foxo1*-Deleted GC B Cells Express LZ-like Genes and Populate GCs Lacking a DZ.

(A) Representative flow cytometry analysis of splenocytes from immunized control and mutant animals (*P110**; *Pten*$^{fl/fl}$; *Foxo1*$^{fl/fl}$) at day 10 after SRBC injection. Cells were consecutively gated as in Figure 1D.

(B) Summary and quantification of flow cytometry data as shown in (A). Each symbol represents an individual animal; horizontal lines indicate the mean.

(C) Summary and quantification of Peyer's patches data (presented as in B).

(D) Hierarchical cluster analysis based on LZ and DZ signature genes (n = 774 probe sets corresponding to n = 584 unique genes). DZ (CD86^{lo}CXCR4^{hi}) and LZ

(CD86^{hi}CXCR4^{lo}) cells of control animals and total GC B cells (CD38^{lo}FAS^{hi}) of *P110**, *Pten*$^{fl/fl}$ and *Foxo1*$^{fl/fl}$ samples were analyzed. Log2 transformed and mean-centered gene expression data are color coded.

(E) Gene set enrichment analysis (GSEA) showing a highly significant enrichment ($p < 0.001$) of the normal DZ transcriptional program in FOXO1-proficient GC B cells (left: positive association of DZ-upregulated genes with FOXO1-proficient cells; right: positive association of LZ-upregulated genes with FOXO1-deficient cells).

(F) Immunofluorescence analysis of spleen sections from immunized control and mutant animals (day 10 after SRBC administration). The same antibodies as in Figure 1C were used. Dashed lines delineate GCs. Two individual animals per genotype were analyzed. Scale bars represent 25 μm.

NS, not significant ($p > 0.05$); *$p \leq 0.05$ and **$p \leq 0.001$ (Wilcoxon-Mann-Whitney test). See also Figure S2 and Table S2.

Figure 3. Normal Proliferation and Survival of PI3K-Pathway-Activated or *Foxo1*-Deleted GC and In Vitro Activated B Cells.

(A) Immunofluorescence analysis of spleen sections from immunized control and mutant animals (day 10 after SRBC injection). Antibodies detecting IgD (expressed on follicular B cells), BCL6 (expressed by GC B cells) and Ki67 were used. Two individual animals per genotype were analyzed. Scale bar represents 25 μm.

(B) Summary and quantification of BrdU incorporation in splenic GC B cells of immunized control and mutant animals (day 10 after SRBC injection and 3 hr after BrdU application). LZ and DZ cells of control animals were included in the analysis. Each symbol represents an individual animal; horizontal lines indicate the mean.

(C) CellTrace analysis in anti-CD40+IL4-stimulated B cells of various genotypes (Control, solid grey line; *P110**, blue line; *Foxo1*$^{fl/fl}$, black line). Day 0 (d0) corresponds to the CellTrace labeling efficiency of the B cells before stimulation. At days 2, 3 and 4 after stimulation, only reporter-positive cells were analyzed. Data are representative of two independent experiments.

(D) Percentage of living B cells after anti-CD40+IL4 stimulation at indicated time points. Data are normalized to the number of cells at day 0 (input). Data are representative of two independent experiments; horizontal lines indicate the mean.

NS, not significant ($p > 0.05$); *$p \leq 0.05$ and **$p \leq 0.001$ (Wilcoxon-Mann-Whitney test). See also Figure S3.

Figure 4. Reduced Mutation Load in the Immunoglobulin Genes of PI3K-Pathway-Activated or *Foxo1*-Deleted GC B cells and Impaired Selection of NP-Specific GC B Cells in Mutant Animals.

(A) J_H4 intron mutation analysis in splenic GC B cells of SRBC-injected animals at day 10 (d10) and day 20 (d20) after immunization. Non-GC B cells of control

animals were included in the analysis. At least two individual animals per genotype were analyzed. Each symbol represents an individual sequence; red horizontal lines indicate the mean.

(B) Quantitative RT-PCR analysis of *Aicda* expression in non-GC and GC B cells of control and mutant animals (day 10 after SRBC immunization). Results are normalized to those of non-GC B cells and are presented relative to expression of the control gene *Hprt*. Each symbol represents an individual animal; horizontal lines indicate the mean.

(C) Label-free quantification of the ILLPLYEVDDLR peptide derived from AID protein in control and mutant GC B cells by LC-MS/MS. AID intensity is normalized to the intensity of HPRT. Each symbol represents an individual sample; horizontal lines indicate the mean. Note: the peptide was not detectable in one out of three *Foxo1* $^{fl/fl}$ samples.

(D and E) Summary and quantification of flow cytometry data of Igλ^+ (D) and hapten-binding reporter$^+$ GC B (E) cells detected in the spleens of immunized control and mutant animals (day 20 after NP-CGG immunization). Each symbol represents an individual animal; horizontal lines indicate the mean.

(F) Pie charts showing the distribution of clones carrying the W33L mutation in *V_H186.2* for each genotype assayed, with the number of individual clones analyzed shown at the center of each pie chart. The assay was performed by PCR and sequencing using the cDNA of single splenic GC B cells isolated from control and mutant mice at day 20 after NP-CGG immunization. Two individual animals per genotype were analyzed.

NS, not significant ($p > 0.05$); *$p \leq 0.05$ and **$p \leq 0.001$ (Wilcoxon-Mann-Whitney test). See also Figure S4.

Figure 5. Co-expression of c-MYC and FOXO1 in a Subset of LZ Cells.

Two examples of spleen sections from immunized control animals (day 10 after SRBC immunization) analyzed by immunofluorescence. Antibodies detecting CD21/CD35 (expressed by the FDC network) (A), c-MYC (A and B) and FOXO1 (A and B) were used. White lines delineate DZ and LZ. Two individual animals were analyzed. Scale bars represent 25 μm (B) Graph**:** Summary and quantification of immunofluorescence analysis. Each symbol represents an individual GC; horizontal line indicates the mean.

Figure 6. CSR Is Controlled by the PI3K Pathway and FOXO1 in GC B Cells.

(A) Representative flow cytometry analysis of splenocytes from immunized control and mutant animals (*P110**; *Pten*$^{fl/fl}$; *Foxo1*$^{fl/fl}$) at day 10 after SRBC injection. Cells were consecutively gated as in Figure 1D.

(B) Summary and quantification of flow cytometry data as shown in (A). Each symbol represents an individual animal; horizontal lines indicate the mean.

(C) Summary and quantification of Peyer's patches data (presented as in B).

(D) Quantitative RT-PCR analysis of μ germline transcript (GLT) expression in splenic GC B cells of control and mutant animals (day 10 after SRBC immunization). Non-GC B cells of control animals were included in the analysis.

Results are normalized to those of control cells and are presented relative to expression of the control gene *Hprt*. Each symbol represents an individual animal; horizontal lines indicate the mean.

(E) Quantitative RT-PCR analysis of γ1 GLT (left) and post-switch transcript (PST; right) expression in splenic GC B cells of control and mutant animals (presented as in D).

NS, not significant ($p > 0.05$); *$p \leq 0.05$ and **$p \leq 0.001$ (Wilcoxon-Mann-Whitney test). See also Figure S5.

Figure 7. PI3K Activation or *Foxo1* Deletion in GC B Cells Interferes with CSR Initiation.

(A) Pie charts showing the distribution of clones carrying the indicated number of mutations in the 820 base pair region immediately upstream of the μ switch (Sμ) region for each genotype assayed, with the number of reads analyzed shown at the center of each pie chart. The assay was performed by PCR and sequencing using the genomic DNA of splenic GC B cells isolated from control and mutant mice at day 10 after SRBC immunization. Non-GC B cells ($B220^{+}CD19^{+}CD38^{hi}FAS^{lo}$) were included in the analysis as a negative control. Data of two animals per genotype are summarized.

(B) For all C:G-targeted somatic mutations in (A), the sequence context of the mutated C base was analyzed for each genotype (non-GC B cells were excluded

from analysis). The percentage of mutations at A:T base pairs versus G:C base pairs is shown for each genotype.

(C) Distribution of Sμ-associated somatic mutations shown in (A).

See also Figure S6.

Figure 1

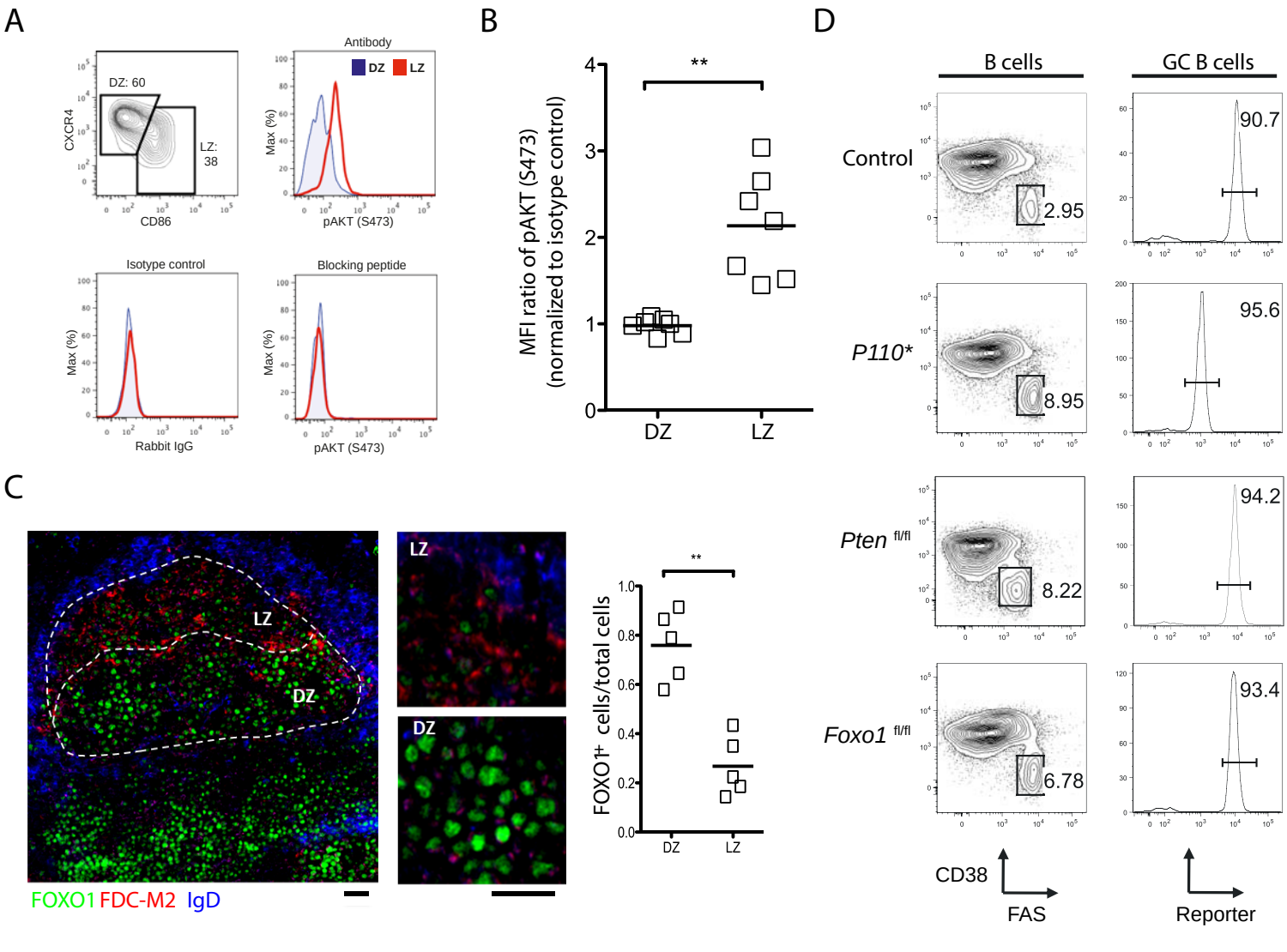
A
DZ: 60
LZ: 38
CXCR4
CD86
Antibody
DZ
LZ
Max (%)
pAKT (S473)
Isotype control
Rabbit IgG
Blocking peptide
pAKT (S473)
B
MFI ratio of pAKT (S473) (normalized to isotype control)
**
DZ
LZ
C
LZ
DZ
FOXO1 FDC-M2 IgD
FOXO1+ cells/total cells
**
DZ
LZ
D
B cells
GC B cells
Control
2.95
90.7
P110*
8.95
95.6
Pten fl/fl
8.22
94.2
Foxo1 fl/fl
6.78
93.4
CD38
FAS
Reporter
E
Reporter+ cells (%) [in GC B cells]
NS
NS
**
Control
P110*
Pten fl/fl
Foxo1 fl/fl
F
GC B cells (%) [in B cells]
NS
**
NS
Control
P110*
Pten fl/fl
Foxo1 fl/fl
G
Reporter+ cells (%) [in GC B cells]
NS
NS
Control
P110*
Foxo1 fl/fl
H
GC B cells (%) [in B cells]
NS
NS
Control
P110*
Foxo1 fl/fl

Figure 2

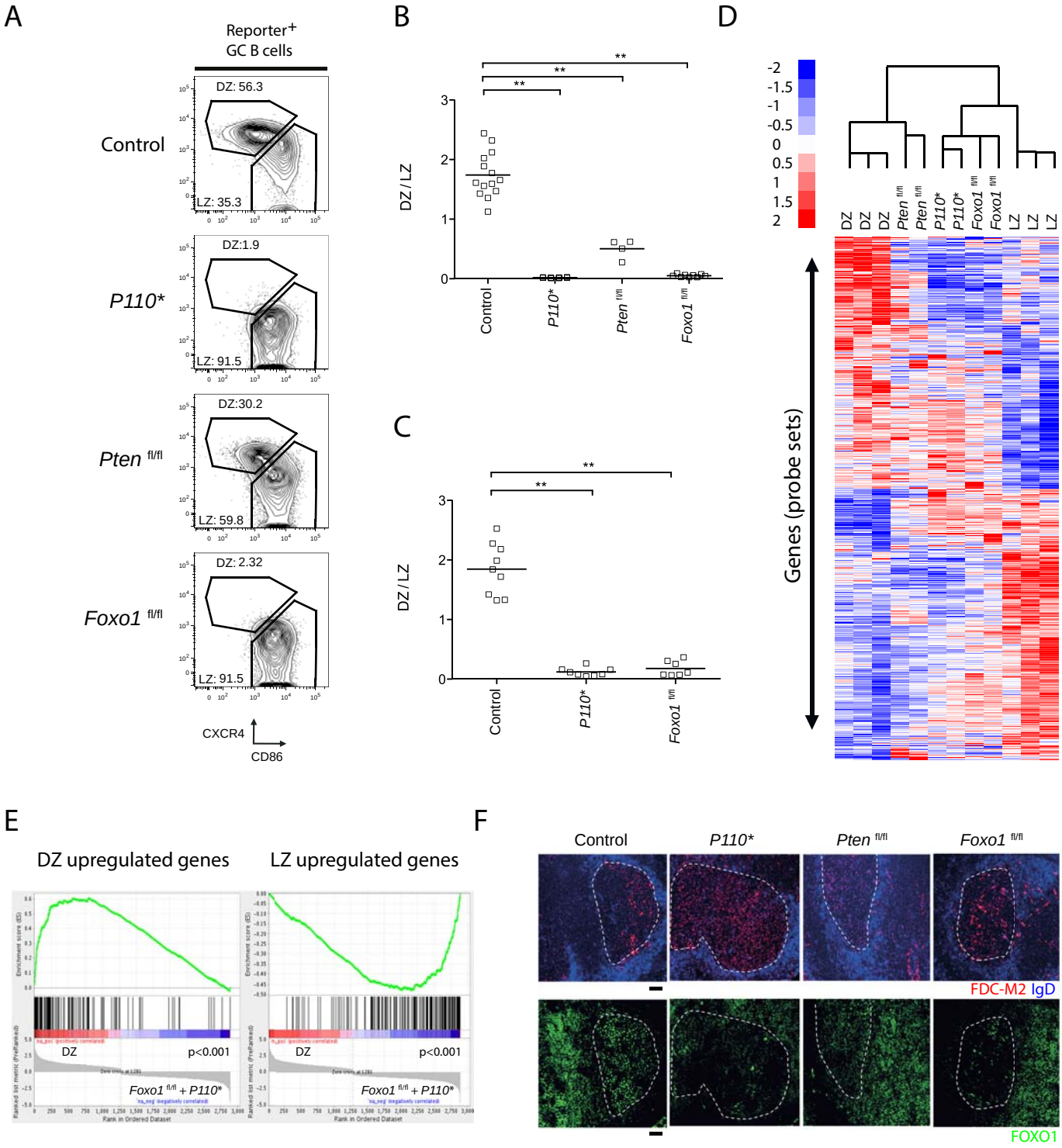
A
Reporter+
GC B cells
Control
DZ: 56.3
LZ: 35.3
P110*
DZ:1.9
LZ: 91.5
Pten fl/fl
DZ:30.2
LZ: 59.8
Foxo1 fl/fl
DZ: 2.32
LZ: 91.5
CXCR4
CD86
B
DZ / LZ
Control
P110*
Pten fl/fl
Foxo1 fl/fl
C
DZ / LZ
Control
P110*
Foxo1 fl/fl
D
Genes (probe sets)
DZ
LZ
E
DZ upregulated genes
LZ upregulated genes
DZ
p<0.001
Foxo1 fl/fl + P110*
F
Control
P110*
Pten fl/fl
Foxo1 fl/fl
FDC-M2 IgD
FOXO1

Figure 3

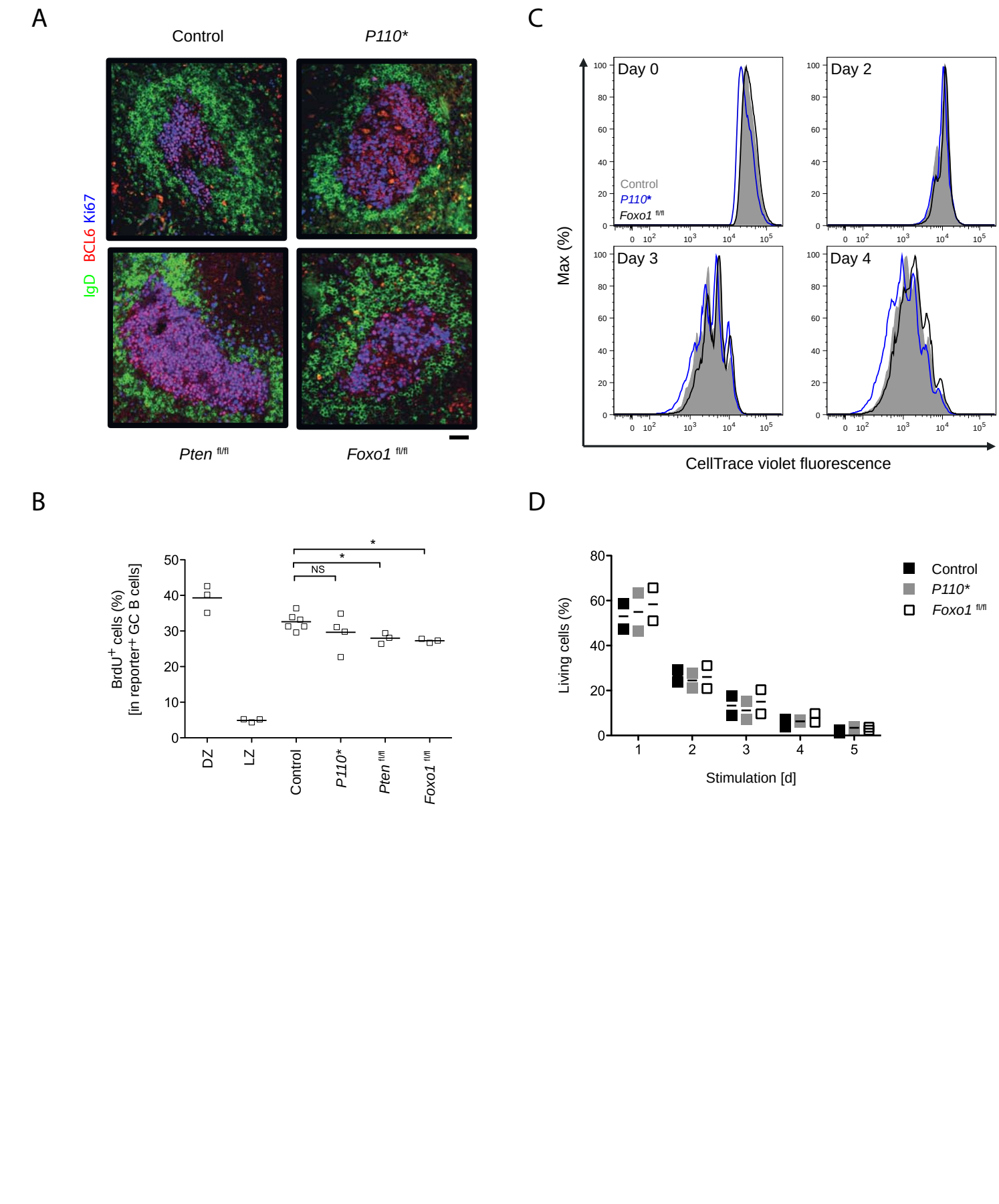
A
Control
P110*
IgD BCL6 Ki67
Pten fl/fl
Foxo1 fl/fl
C
Day 0
Day 2
Day 3
Day 4
Control
P110*
Foxo1 fl/fl
Max (%)
CellTrace violet fluorescence
B
BrdU+ cells (%)
[in reporter+ GC B cells]
NS
*
*
DZ
LZ
Control
P110*
Pten fl/fl
Foxo1 fl/fl
D
Living cells (%)
Stimulation [d]
Control
P110*
Foxo1 fl/fl

Figure 4

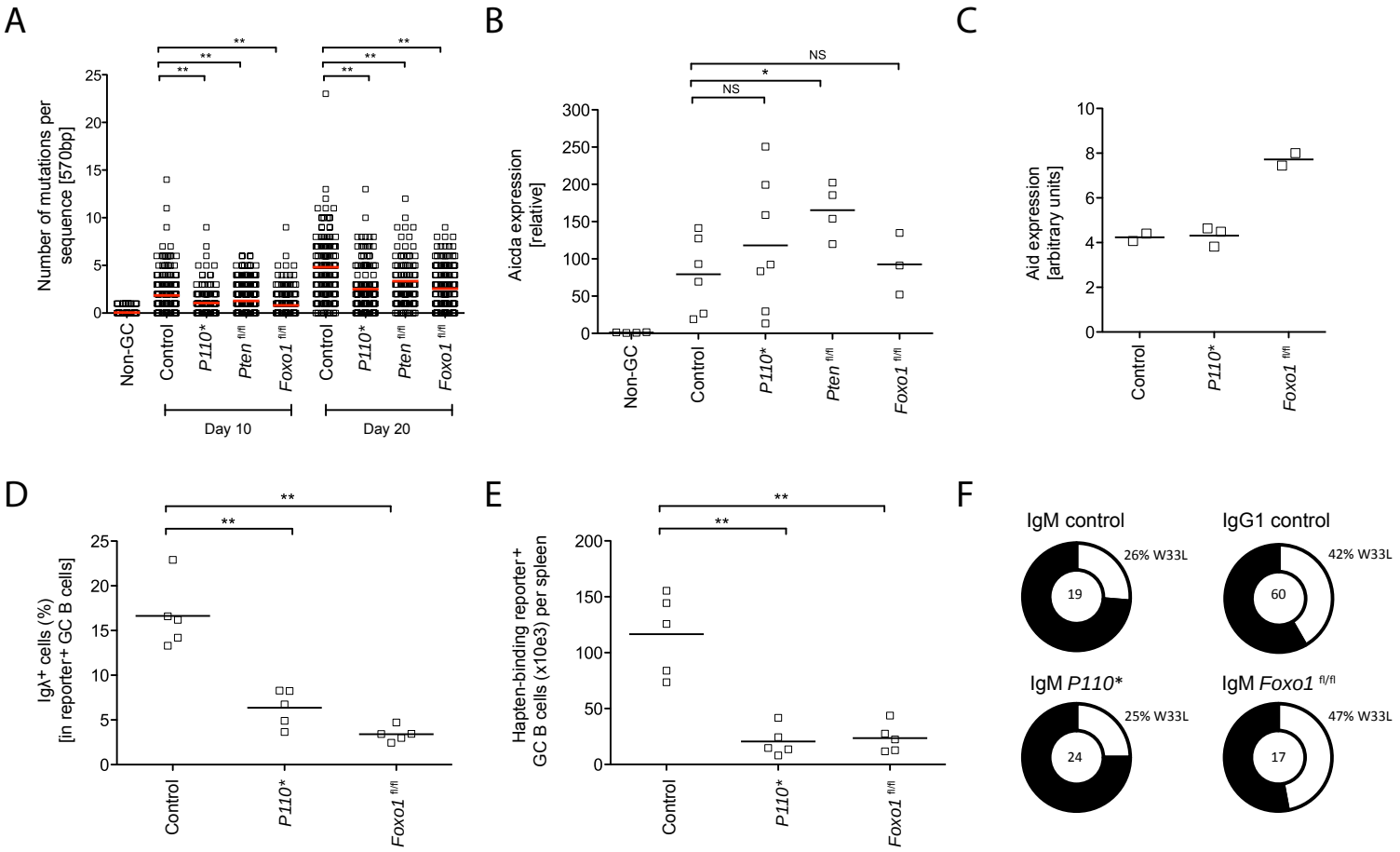
A
Number of mutations per sequence [570bp]
Non-GC
Control
P110*
Pten fl/fl
Foxo1 fl/fl
Day 10
Day 20
B
Aicda expression [relative]
NS
C
Aid expression [arbitrary units]
D
IgA+ cells (%) [in reporter+ GC B cells]
E
Hapten-binding reporter+ GC B cells (x10e3) per spleen
F
IgM control
26% W33L
19
IgG1 control
42% W33L
60
IgM P110*
25% W33L
24
IgM Foxo1 fl/fl
47% W33L
17

Figure 5

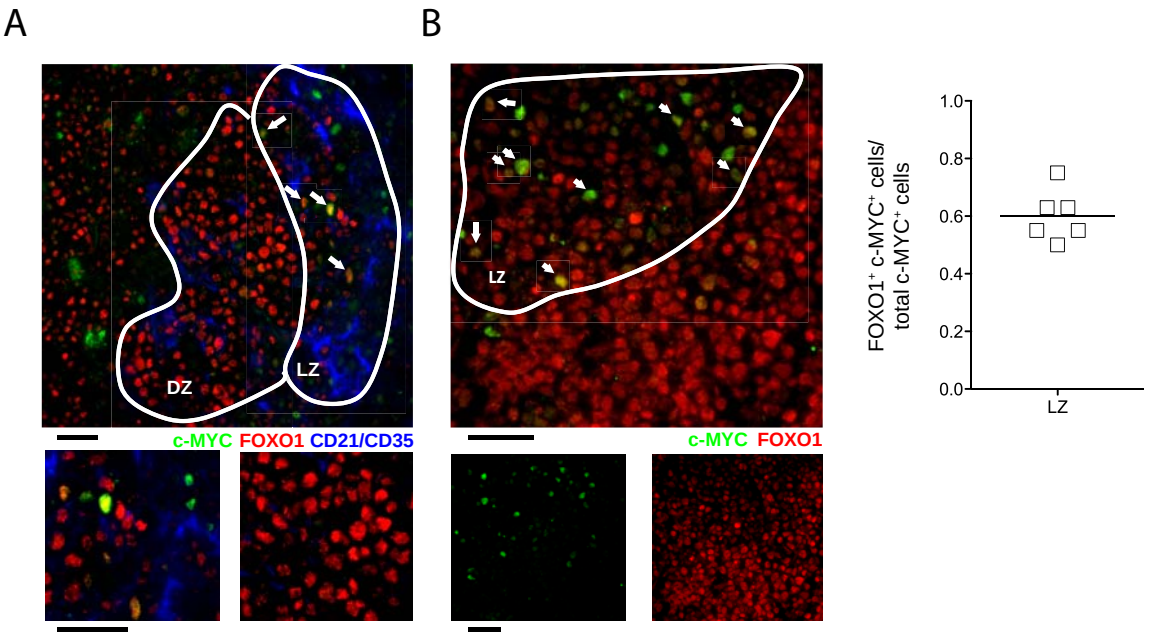
A
B
DZ
LZ
LZ
c-MYC FOXO1 CD21/CD35
c-MYC FOXO1
FOXO1⁺ c-MYC⁺ cells/
total c-MYC⁺ cells
1.0
0.8
0.6
0.4
0.2
0.0
LZ

Figure 6

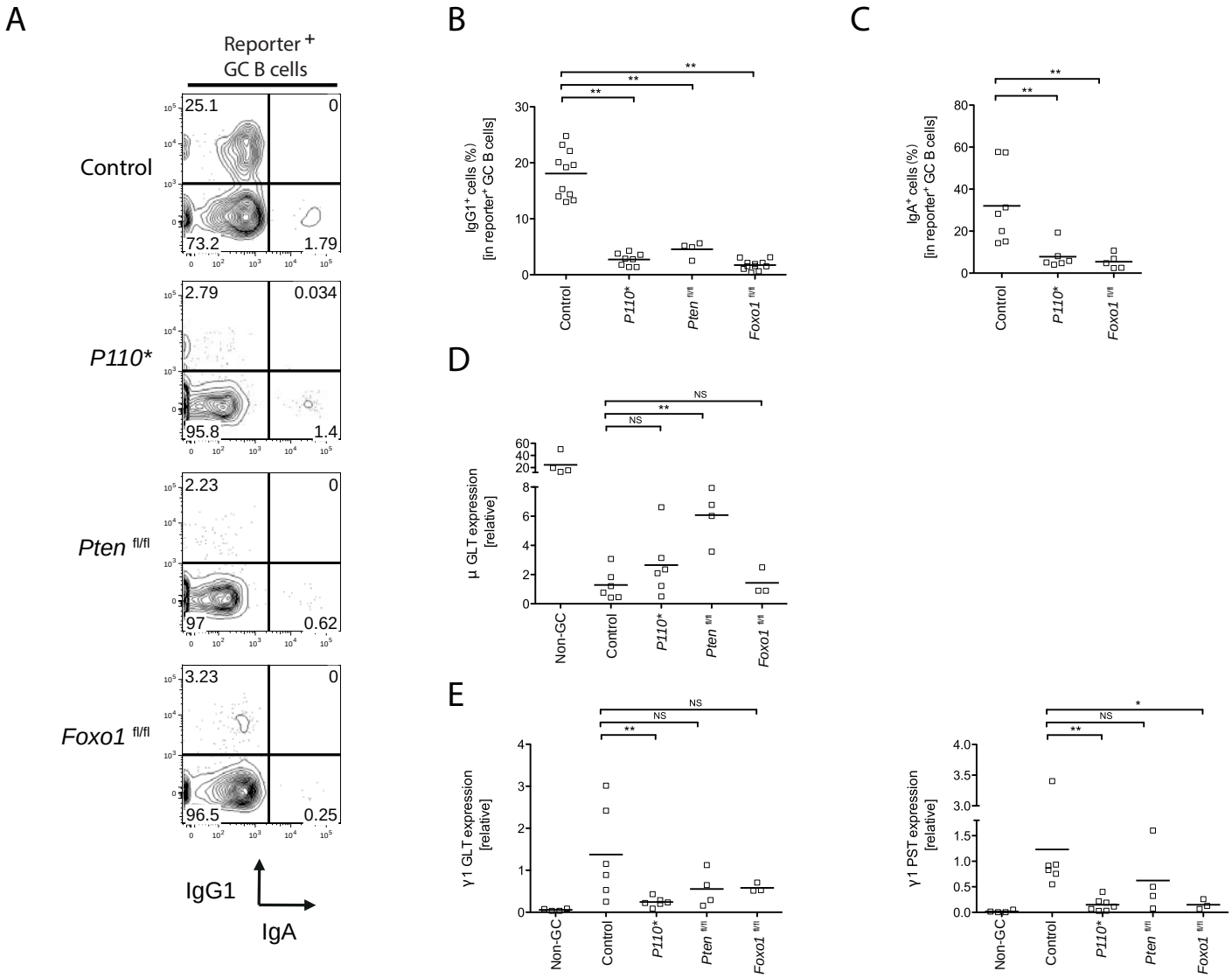
A
Reporter + GC B cells
Control
P110*
Pten fl/fl
Foxo1 fl/fl
25.1
0
73.2
1.79
2.79
0.034
95.8
1.4
2.23
0
97
0.62
3.23
0
96.5
0.25
IgG1
IgA
B
IgG1+ cells (%) [in reporter+ GC B cells]
Control
P110*
Pten fl/fl
Foxo1 fl/fl
C
IgA+ cells (%) [in reporter+ GC B cells]
D
μ GLT expression [relative]
Non-GC
E
γ1 GLT expression [relative]
γ1 PST expression [relative]
NS

Figure 7

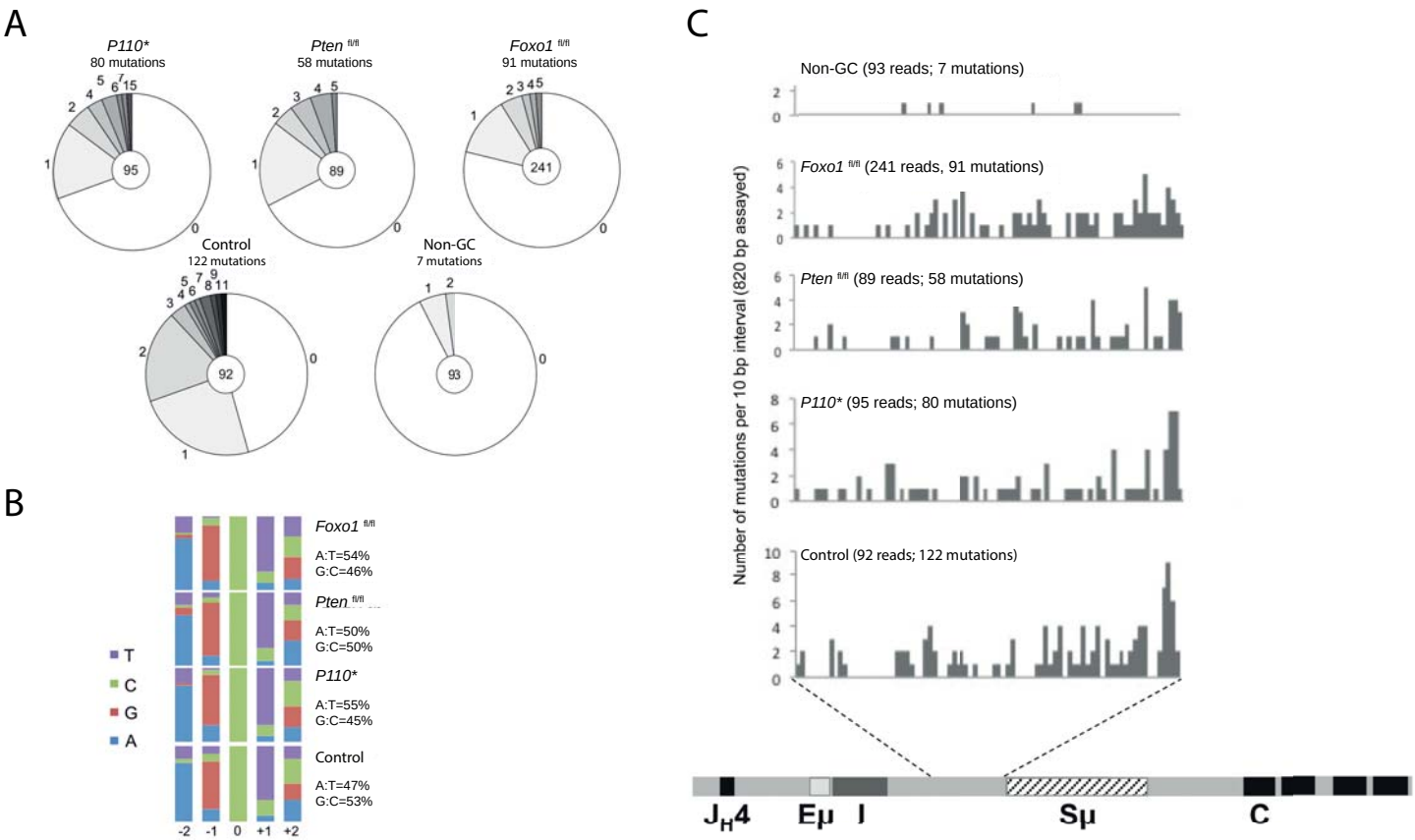
A
P110*
80 mutations
95
Pten fl/fl
58 mutations
89
Foxo1 fl/fl
91 mutations
241
Control
122 mutations
92
Non-GC
7 mutations
93
B
T
C
G
A
Foxo1 fl/fl
A:T=54%
G:C=46%
Pten fl/fl
A:T=50%
G:C=50%
P110*
A:T=55%
G:C=45%
Control
A:T=47%
G:C=53%
-2
-1
0
+1
+2
C
Non-GC (93 reads; 7 mutations)
Foxo1 fl/fl (241 reads, 91 mutations)
Pten fl/fl (89 reads; 58 mutations)
P110* (95 reads; 80 mutations)
Control (92 reads; 122 mutations)
Number of mutations per 10 bp interval (820 bp assayed)
JH4
Eμ
I
Sμ
C